Inorg. Chem. **2003**, *42*, 7544–7549

Bulk Spontaneous Magnetization in the New Radical Cation Salt TM-TTF[Cr(NCS)$_4$(isoquinoline)$_2$] (TM-TTF = Tetramethyltetrathiafulvalene)

M. Mas-Torrent,[†] S. S. Turner,*[,‡] K. Wurst,[§] J. Vidal-Gancedo,[†] X. Ribas,[†] J. Veciana,[†] P. Day,*[,‡] and C. Rovira*[,†]

Institut de Ciència de Materials de Barcelona (CSIC), Campus Universitari de Bellaterra, 08193 Bellaterra, Catalunya, Spain, The Royal Institution of Great Britain, Davy-Faraday Research Laboratory, 21 Albemarle Street, London, W1S 4BS U.K., and Institut für Allgemeine Anorgan. und Theoret. Chemie, Universitat Innsbruck, Innrain 52a, A-6020 Innsbruck, Austria

Received April 9, 2003

A new organic–inorganic hybrid salt [TM-TTF][Cr(NCS)$_4$(isoquinoline)$_2$] (**1**) (TM-TTF = Tetramethyltetrathiafulvalene) has been synthesized. Compound **1** crystallizes in the triclinic $P\bar{1}$ space group with $a = 8.269(1)$, $b = 10.211(2)$, and $c = 11.176(2)$ Å, $\alpha = 89.244(9)$, $\beta = 88.114(6)$, and $\gamma = 74.277(7)°$, $V = 907.6(3)$ Å^3, and $Z = 1$. The crystal structure was resolved in the temperature range between 223 and 123 K, showing that changes in the crystal structure at low temperature result in stronger interactions between anions and cations. The packing of **1** consists of mixed anion–cation layers in the *bc* plane containing S···S and π–π anion–cation interactions, the layers being connected by very short S···S contacts between anions and cations. Magnetic measurements in a small external field show bulk spontaneous magnetization with a T_c of 6.6 K consistent with the presence of weakly coupled ferrimagnetic order in compound **1**. The EPR measurements also demonstrate the interaction between the d and π electrons and the presence of an internal magnetic field brought about by the magnetic ordering.

Introduction

Since the discovery of the first organic metal in 1972,[1] great efforts have been devoted to preparing new conducting charge transfer salts based on tetrathiafulvalene or its analogues, resulting in a wide range of conductors. Until relatively recently the interest in this class of compounds was focused exclusively on their transport properties, but another interesting approach is to use radical donors as building blocks for π-electron-based low-dimensional magnets, which has led to 1D and 2D antiferromagnets and spin-ladders.[2−4] In the past few years, special emphasis has been placed on the combination of different physical properties such as conductivity and magnetism. The magnetic properties are typically introduced by employing anionic complexes with paramagnetic centers. This strategy has given rise to, among other interesting salts, the first molecular superconductor containing paramagnetic metal ions, β''-(BEDT-TTF)$_4$[(H$_3$O)Fe(C$_2$O$_4$)$_3$]C$_6$H$_5$CN,[5] and to the first molecular-based compound exhibiting both ferromagnetism and metallic conductivity.[6] For the majority of such compounds the coexisting magnetic and electrical transport properties originate from independent networks in which the magnetic order is not mediated by the radical donor. Recently, our group has prepared TTF-based salts with strong donor−acceptor interactions and subsequent long-range ferrimagnetic order. This has been achieved by using anions of the type [Cr(NCS)$_4$(N-donor)$_{1,2}$]$^-$, where N-donor = 1,10′-phenantroline

* To whom correspondence should be addressed. E-mail: cun@icmab.es (C.R.); profpday@msn.com (P.D.); sst@ri.ac.uk (S.T.).
† Institut de Ciència de Materials de Barcelona (CSIC).
‡ The Royal Institution.
§ Universitat Innsbruck.

(1) Ferraris, J.; Cowan, D. O.; Walatka, V. V.; Perlstein, J. H. *J. Am. Chem. Soc.* **1973**, *95*, 948.
(2) Guionneau, P.; Gaultier, J.; Rahal, M.; Bravic, G.; Mellado, J. M.; Chasseau, D.; Ducasse, L.; Kurmoo, M.; Day, P. *J. Mater. Chem.* **1995**, *5*, 1639.
(3) Enoki, T.; Yamaura, J.-I.; Miyazaki, A. *Bull. Chem. Soc. Jpn.* **1997**, *70*, 2005.
(4) Rovira, C. *Chem. Eur. J.* **2000**, *6*, 1.
(5) (a) Graham, A. W.; Kurmoo, M.; Day, P. *J. Chem. Soc., Chem. Commun.* **1995**, 2061. (b) Kurmoo, M.; Graham, A. W.; Day, P.; Coles, S. J.; Hursthouse, M. B.; Caufield, J. L.; Singleton, J.; Pratt, F. L.; Hayes, W.; Ducasse, L.; Guionneau, P. *J. Am. Chem. Soc.* **1995**, *117*, 12209.
(6) Coronado, E.; Galán-Mascarós, J. R.; Goméz-García, C. J.; Laukhin, V. *Nature* **2000**, *408*, 447.

10.1021/ic034379c CCC: $25.00
Published on Web 10/11/2003

or isoquinoline.[7,8] The anions were designed specifically to promote π-stacking and S···S close contacts between the anion and the radical donor. A common characteristic of these salts is the formation of stacks of alternating cations and anions, so the observation of magnetic order can be rationalized by antiferromagnetic exchange between the cation and anion-based spins. The combination of this type of anion with BDH-TTP (2,5-bis(1,3-dithiolan-2-ylidene)-1,3,4,6-tetrathiapentalene) also gave salts with magnetic order.[9] Among this family of compounds, the salt (TTF)-[Cr(NCS)$_4$(1,10′-phenanthroline)] exhibits the highest T_c at 9 K.[8] In our continuing pursuit of new magnetic materials using this new methodology, we present the preparation and properties of a new salt of the donor TM-TTF, tetramethyltetrathiafulvalene, and the anion [Cr(NCS)$_4$(isoquinoline)$_2$]$^-$.

Experimental Section

Synthesis. The synthesis of the donor TM-TTF was carried out by adapting the Wittig-like coupling with triethylamine as reported in the literature.[10] The salt [C_9H_8N][Cr(NCS)$_4$(C_9H_7N)$_2$], where C_9H_7N is isoquinoline, was prepared by a ligand exchange reaction with Reinecke's salt, NH$_4$[Cr(NCS)$_4$(NH$_3$)$_2$], on adding the corresponding nitrogen donor ligand and refluxing in ethanol overnight.[7]

The salt **1** was synthesized by electrochemical crystallization in freshly distilled dichloromethane in conventional H-shaped electrochemical cells with Pt electrodes at a constant temperature of 295(2) K and at a constant current of 1 μA over 1 week. A suspension of 8 mg of [C_9H_8N][Cr(NCS)$_4$(C_9H_7N)$_2$] in 12 mL of dichloromethane was prepared, and during stirring 18-crown-6-ether was added slowly until the anion completely dissolved. A 4 mg amount of solid TM-TTF was placed on the anode arm, and the remainder of the cell was filled with the Cr complex solution. Black crystals forming amorphous clusters were grown on the anode. By separating them, it was possible to get suitable crystals for X-ray diffraction, and the product was found to be [TM-TTF][Cr(NCS)$_4$-(C_9H_7N)$_2$], **1**.

Crystallographic Data Collection and Structure Determination. X-ray diffraction data were collected at five different temperatures between 213 and 123 K, on a Nonius Kappa CCD diffractometer with monochromatic Mo Kα radiation (λ = 0.710 73 Å). All data sets have been collected under similar conditions with the same φ-scan rotation of the crystal and the equal time for the measured frames. Complete crystallographic data is given for 213 and 123 K experiments in Table 1. The relevant crystallographic parameters for the five temperature data sets are given in Table 2. Intensities were integrated using DENZO and scaled with SCALEPACK. The structures were solved with direct methods SHELXS86 and refined against F^2 with SHELX93. Hydrogen atoms at carbon atoms were added geometrically and refined using a riding model. All non-hydrogen atoms were refined with anisotropic displacement parameters.

Table 1. Crystallographic Data for **1** at 213 and 123 K

param	213(2) K	123(2) K
chem formula	$C_{32}H_{26}CrN_6S_8$	$C_{32}H_{26}CrN_6S_8$
fw	803.07	803.07
λ, Å	0.71073, Mo Kα	0.71073, Mo Kα
space group	$P\bar{1}$ (No. 2)	$P\bar{1}$ (No. 2)
a, Å	8.269(1)	8.112(6)
b, Å	10.211(2)	9.886(6)
c, Å	11.176(2)	11.507(9)
α, deg	89.244(9)	83.89(5)
β, deg	88.114(6)	82.37(3)
γ, deg	74.227(7)	76.34(6)
V, Å^3	907.6(3)	886.1(11)
Z	1	1
ρ_{calcd}, g cm^{-3}	1.469	1.505
μ, cm^{-1}	8.08	8.28
reflcns collcd	2849	2493
reflcns $I > 3\sigma(I)$	1340	1007
indepdt reflcns	1629	1562
$R(F_o)$	0.0331	0.0636
$R_w(F_o^2)$	0.0725	0.1379

Table 2. Comparative Crystallographic Data for Compound **1** for Collections between 213 and 123 K

temp (K)	lattice consts, Å and deg			*V* (Å^3)	*R*-value (%)	mosaicity
	a, α	*b*, β	*c*, γ			
213	8.269(1)	10.211(2)	11.176(2)	907.7(2)	3.31	0.76
	89.244(9)	88.114(9)	74.227(7)			
187	8.262(1)	10.216(2)	11.141(2)	904.3(2)	3.18	0.83
	89.338(9)	88.175(8)	74.195(7)			
161	8.255(1)	10.217(2)	11.117(2)	901.5(2)	3.07	0.95
	89.416(9)	88.257(9)	74.147(7)			
130	8.242(2)	10.214(3)	11.071(3)	896.2(4)	4.51	1.66
	89.59(2)	88.46(2)	74.14(1)			
123	8.112(6)	9.886(6)	11.507(9)	886.1(11)	6.36	2.54
	83.89(5)	82.37(3)	76.34(6)			

Physical Property Measurements. Dc and ac magnetic measurements of polycrystalline and randomly orientated samples of **1**, held in gelatine capsules inside a plastic tube, were measured using a Quantum Design MPMS7 SQUID magnetometer or an Oxford Instruments MagLab 2000 with ac probe, respectively. The data were measured on warming. All samples were field cooled, and the cooling field were identical to the measuring fields. The core diamagnetism was estimated for each of the salts by using Pascal's constants. Electron paramagnetic resonance (EPR) spectra were obtained from polycrystalline and randomly orientated samples with a Bruker X-band ESP 300E spectrometer equipped with a rectangular cavity operating in the TE102 mode. Spectra were taken in the 2−300 K range using a Bruker variable-temperature unit and an Oxford Instruments EPR-900 cryostat, a field frequency lock ER 033M system, and an NMR gaussmeter ER 035M.

Results and Discussion

Crystal Structures. The crystal structure was solved at five different temperatures in a range between 213 and 123 K. From the crystallographic data shown in Table 2 there is clearly a phase transition at 123 K, since the cell volume decreases smoothly on lowering the temperature and then there is a sharp decrease from 130 to 123 K. At 123 K we observe a significant change of the lattice constants since the *a* and *b* axes contract but the *c* axis elongates. Thus, the complete structural description that follows focuses on the structures at the highest and lowest temperatures of the range measured (i.e. 213 and 123 K).

(7) (a) Turner, S. S.; Michaut, C.; Durot, S.; Day, P.; Gelbrich, T.; Hurtshouse, M. B. *J. Chem. Soc., Dalton Trans.* **2000**, 905. (b) Setifi, F.; Golhen, S.; Ouahab, L.; Turner, S. S.; Day, P. *Cryst. Eng. Commun.* **2002**, *1*, 1.

(8) Turner, S. S.; Le Pevelen, D.; Day, P.; Prout, K. *J. Chem. Soc., Dalton Trans.* **2000**, 2739.

(9) (a) Miyazaki, A.; Okabe, K.; Enoki, T.; Setifi, F.; Golhen, S.; Ouahab, L.; Toita, T.; Yamada, J. *Synth. Met.* **2003**, *137*, 1195. (b) Setifi, F.; Golhen, S.; Ouahab L.; Miyazaki, A.; Okabe, K.; Enoki, T.; Toita, T.; Yamada, J. *Inorg. Chem.* **2002**, *41*, 3786.

(10) (a) Bechgaard, K.; Cowan, D.; Bloch, A. N.; Henriksen, L. *J. Org. Chem.* **1975**, *40*, 746. (b) Chiang, L.-Y.; Shu, P.; Holt, D.; Cowan, D. *J. Org. Chem.* **1983**, *48*, 4713. (c) Gonella, N. C.; Cava, M. P. *J. Org. Chem.* **1978**, *43*, 369. (d) Llacay, J.; Mata, I.; Molins, E.; Veciana, J.; Rovira, C. *Adv. Mater.* **1998**, *3*, 330.

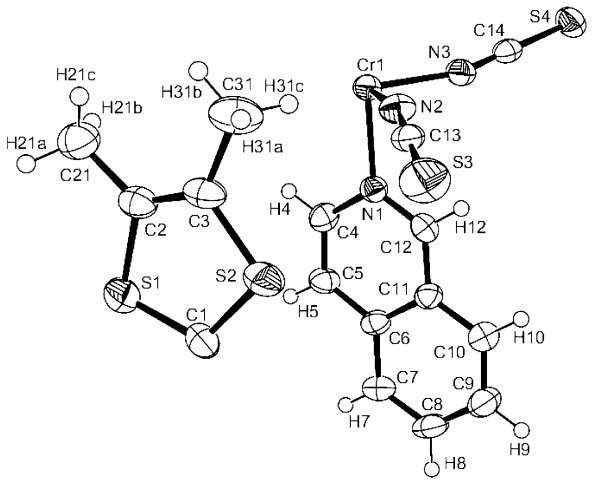

Figure 1. ORTEP diagram of the asymmetric unit of **1** showing the atom numbering scheme and 50% thermal ellipsoids.

Table 3. Selected Bond Lengths (Å) and Angles (deg) for Complex [TM-TTF][$Cr(NCS)_4$(isoquinoline)$_2$] at 213 K and at 123 K (in Brackets)

bond	dist, Å	bond	dist, Å
Cr1−N1	2.089(3) [2.077(7)]	S2−C1	1.712(4) [1.726(10)]
Cr1−N2	1.988(4) [1.989(10)]	S2−C3	1.737(5) [1.737(10)]
Cr1−N3	1.982(4) [1.970(9)]	C1−C1	1.382(8) [1.37(2)]
S1−C1	1.715(4) [1.715(11)]	C2−C3	1.341(6) [1.331(14)]
S1−C2	1.733(4) [1.746(10)]		

bond	angle, deg	bond	angle, deg
N1−Cr1−N2	89.77(14) [90.0(3)]	N2−Cr1−N3	89.06(14) [89.5(3)]
N1−Cr1−N3	91.56(13) [91.3(3)]	S1−C1−S2	114.3(2) [113.7(5)]
N2−Cr1−N3	90.94(14) [90.5(3)]	C1−S1−C2	96.8(2) [96.5(5)]
Cr1−N2−C13	163.2(4) [159.1(8)]	C1−S2−C3	96.2(2) [96.7(5)]
Cr1−N3−C14	163.9(3) [157.7(8)]	S1−C2−C3	115.7(3) [116.6(9)]
N2−C13−S3	179.2(4) [178.5(10)]	S2−C3−C2	116.9(3) [116.3(8)]
N3−C14−S4	179.4(4) [178.9(9)]	C1−C1−S2	123.3(4) [123.3(12)]
N1−Cr1−N2	90.23(14) [90.0(3)]	C1-C1−S1	122.4(4) [123.0(11)]
N1−Cr1−N3	88.44(13) [88.7(3)]		

A standard ORTEP[11] diagram of the asymmetric unit at 213 K is given in Figure 1 showing the labeling scheme and 50% thermal ellipsoids. The crystal and refinement data are given in Table 1, and selected bond distances and angles, in Table 3.

The asymmetric unit contains half-anion and half-cation molecules. The coordination environment around the Cr center is almost octahedral with six Cr−N bonds, where the four bonds to the NCS groups are slightly shorter than those to the isoquinoline ligands; the average Cr−NCS distance at 213 K is 1.985 Å whereas Cr−N(isoquinoline) is 2.089 Å. The same bonds are slightly shortened at 123 K, being 1.980 and 2.077 Å, respectively. The structure at low temperatures also shows a slightly smaller Cr−N−C angle in the anion molecules, 159.1° compared to the 163.3° at 213 K, which at the same time results in a contraction of the anion Cr−NCS arms, with a Cr···S distance of 4.71 Å at 213 K and 4.68 Å at 123 K.

The crystal structure of **1** consists of alternating layers of anions and cations propagated in the *c* direction, as seen in the crystal packing diagram (Figure 2). Unlike most TTF-based salts,[12] the shortest interionic atomic contacts in this salt are between the cation and anion rather than between identical ions. In fact, there is no face to face stacking of the donors and the shortest S···S distance between donors along the *a* axis is 4.27 Å at 213 K and 4.36 Å at 123 K. By contrast, there are two S···S very short contacts between each donor cation and the NCS residues of the surrounding anions, far below the sum of the S van der Waals distances (3.6 Å); S1···S4 is 3.42 Å at 213 K and 3.32 Å at 123 K. However, other longer S···S contacts exist between cations and anions, all of them above 3.76 Å (S2···S3 contact at 213 and 123 K), highlighting the shortening of the S2···S4 contact from 4.32 Å at 213 K to 3.84 Å at 123 K. In addition, there is clear evidence of $\pi-\pi$ stacking between the anion and cation molecules since at 213 K the shortest distance between TM-TTF and the isoquinoline ligand is 3.61 Å for C1···C7 (3.69 Å at 123 K) and the dihedral angle between the mean planes of tetrahiafulvalene and isoquinoline rings is just 2.6(1)°. At 123 K, the shortest distance is between atoms S1 and C8, being 3.63 Å (3.91 Å at 213 K), due to an increased torsion of the donor molecule, yielding an equivalent dihedral angle of 11.2(3)°, which in turn causes a change in the

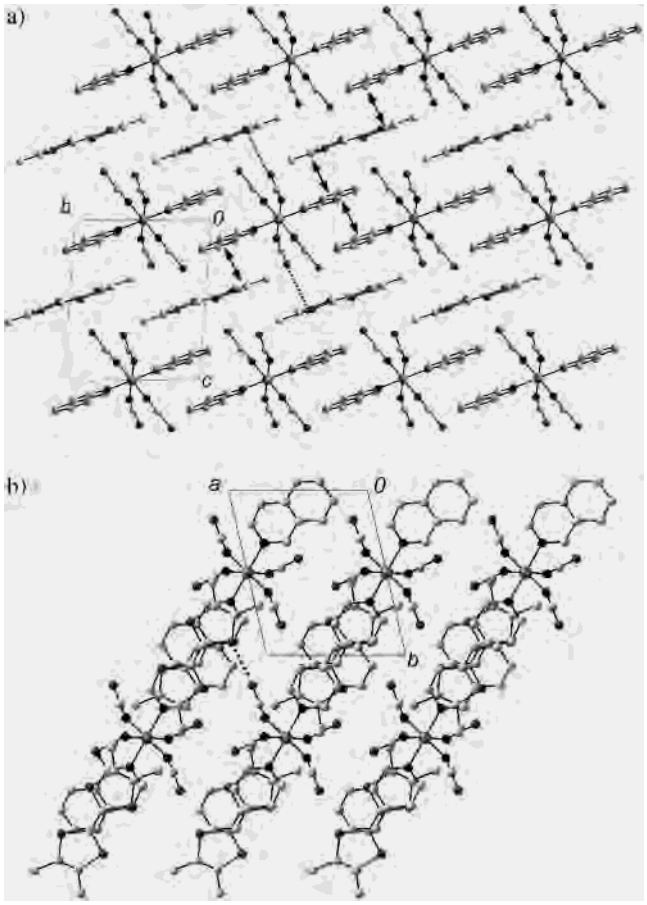

Figure 2. Crystal packing of **1** at 213 K viewed along (a) the crystallographic *a* axis and (b) the crystallographic *c* axis. Dashed lines indicate the short S···S contacts, and the arrows, the $\pi-\pi$ interactions.

(11) Johnson, C. K. *ORTEP*; Report ORNL-5138; Oak Ridge National Laboratory: Oak Ridge, TN, 1976. Farrugia, L. J. *J. Appl. Chem.* **1997**, *30*, 565.

(12) Williams, J. M.; Ferraro, J. R.; Thorn, R. J.; Carlson, K. D.; Geiser, U.; Wang, H. H.; Kini, A. M.; Whangbo, M. H. *Organic Superconductors (Including Fullerenes) Synthesis, Structure, Properties and Theory*; Prentice-Hall: Englewood Cliffs, NJ, 1992.

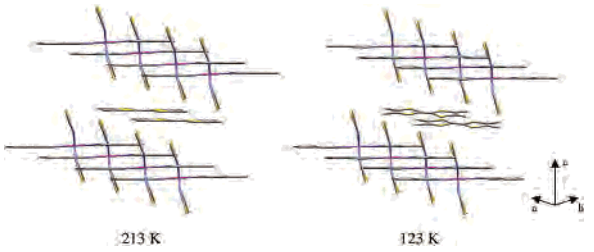

Figure 3. Structural change of **1** when lowering the temperature showing the TM-TTF torsion.

Table 4. Selected Distances (Å) for Complex [TM-TTF][Cr(NCS)$_4$(isoquinoline)$_2$] at 213 K and at 123 K (Distances in Parentheses)

cation−anion intralayer dist, Å		cation−anion interlayer dist, Å	
2 × (S1···S4)	4.079 (3.998)	2 × (S1···S4)	3.416 (3.322)
2 × (S2···S3)	3.763 (3.763)	2 × (S2···S4)	4.314 (3.838)
2 × (H21b−S4)	2.854 (2.926)	2 × (H31b−S3)	2.989 (2.957)

shortest isoq−isoq intralayer $\pi-\pi$ dist, Å		interlayer dist between anion−anion, Å	
2 × (C7···C11)	3.588 (3.514)	2 × (H5···S4)	2.947 (2.929)
		2 × (S4···H5)	2.947 (2.929)

shortest alternating cation−anion intralayer $\pi-\pi$ dist, Å		shortest interlayer cation−cation dist, Å	
2 × (C1···C7)	3.606 (3.690)	S1···S1	4.267 (4.357)

π-stacking interaction when lowering the temperature. In fact, the cations are twisted by 12° at the lower temperature compared to their position at 213 K, and all them lie in the same plane along the *a* axis at 123 K (Figure 3).

The TM-TTF twist also contributes to a deviation in the crystallographic α and β values of about 6° each and leads to stresses in the crystal and to a higher crystal mosaicity. Higher *R* values for the lower temperature measurements are obtained as a consequence (see Table 2). To exclude artifacts in the crystallography results, the crystal was measured some weeks after the first experiments, this time at 118 K, and almost identical lattice constants were obtained. Finally, anion molecules interact through π-stacking of the isoquinoline ligands with the shortest distances between aromatic planes of neighbor anions being 3.51 Å at 123 K and 3.58 Å at 213 K. Due to symmetry requirements the angle formed by the planes of these ligands is trivially 0°. Taking into account all the S···S contacts and $\pi-\pi$ interactions, the crystal structure of compound **1** can be described as *layers* of interacting cation−anion molecules in the *bc* plane. Figure 2 shows that zigzag D−A−D−A chains are formed in the $b + c$ direction by $\pi-\pi$ interactions. These chains are interconnected both by A−A−D−A−A−D $\pi-\pi$ interactions propagating along *b* axis and by S···S contacts along *b*−*c* direction. Layers are connected along *b* by the very short S1···S4 contact. Table 4 collects selected interlayer and intralayer distances.

Of the previously described TTF-based radical ion salts with the same anions as **1**, [BEDT-TTF][Cr(NCS)$_4$(isoquinoline)$_2$] has the most similar structure.[7] The BEDT-TTF salt exhibits bulk ferrimagnetism via antiferromagnetic exchange between the donor radical spin and the acceptor spin on the Cr ion. In comparison to compound **1**, S···S

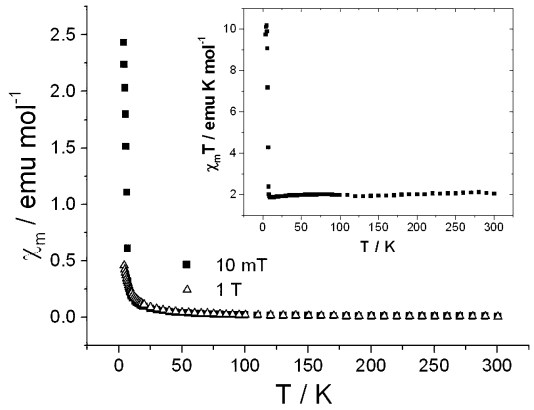

Figure 4. χ_m versus *T* for compound **1** with an external field of 10 mT and 1 T. The inset shows the $\chi_m T$ versus *T* curve with an external field of 10 mT.

contacts exist between BEDT-TTF ions, which are not observed between TM-TTF ions. Furthermore, the interplanar $\pi-\pi$ distance between BEDT-TTF and isoquinoline ligands is much shorter (3.41 Å) than the distance between TM-TTF and isoquinoline in **1** (3.69 Å) at 120 K. This greatly affects the magnetic properties of the compound **1** and accounts for a weaker $\pi-$d interaction as described in the following section.

Physical Properties. The electrical conductivity of **1** was measured as a compressed pellet and was found to be an insulator, which is expected since the TM-TTF molecules are well isolated.

The $\chi_m T$ versus *T* curve with an external field of 10 mT is shown in Figure 4 (inset), where χ_m is the molar magnetic susceptibility and *T* is the measurement temperature. It can be noted that around 120 K, where the phase transition was observed by X-ray diffraction, a very smooth anomaly is barely seen in the $\chi_m T$ versus *T* curve. The general appearance of the curve is what would be expected for a ferrimagnet. A plot of χ_m^{-1} versus *T* gives a straight line at high temperatures (above 10 times T_c, i.e., 66 K; see below), and there is a negative Weiss constant θ of −4.6, showing relatively weak short-range antiferromagnetic coupling between the anion ($S = 3/2$) and donor ($S = 1/2$) spins. The value of the Curie constant is 2.07 emu K mol^{-1}, slightly lower than expected for completely noninteracting Cr(III) ($S = 3/2$) and TM-TTF ($S = 1/2$) (expected $C = 2.23$ emu K mol^{-1} using $g = 1.99$ as measured below). At 10.8 K there is a minimum in $\chi_m T$ (1.84 emu K mol^{-1}) followed by a sharp increase to 10.2 emu K mol^{-1} below the T_c. By contrast the experiment in an external field of 1 T (Figure 4) shows no indication of magnetic order and the data fit very well to the Curie−Weiss law over the whole temperature range with $C = 2.3$ emu K mol^{-1} and $\theta = -1.1$ K. An explanation is that this modest field is sufficient to decouple the weak interaction between the two spin centers, essentially giving a field induced paramagnet. The weak nature of the interaction is evident from the small negative value of θ, as compared to that of the ferrimagnet (TTF)[Cr(NCS)$_4$(1,10′-phenanthroline)],[8] for which $\theta = -24.9$ K, or that of the weak ferromagnet (BDH-TTP)[Cr(NCS)$_4$-(isoquinoline)$_2$],[9] which has $\theta = -20.4$ K. In the former case

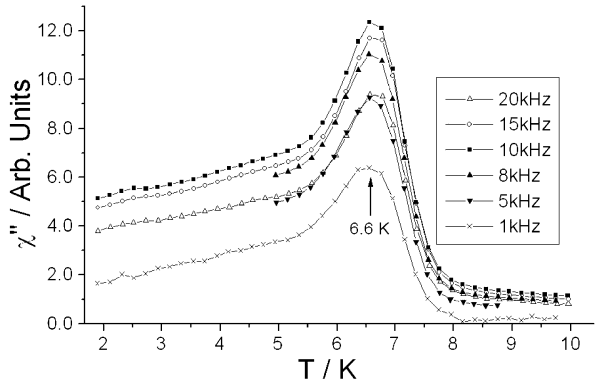

Figure 5. Imaginary component of the ac magnetic susceptibility versus temperature with a drive field of 1 Oe at a range of frequencies.

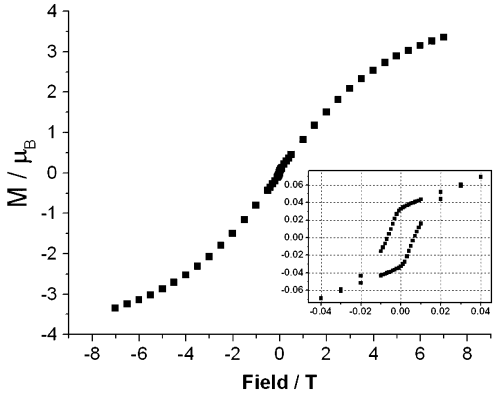

Figure 6. Magnetization versus applied field at 2 K. The inset shows the hysteresis loop about zero field.

Mori et al estimated the strength of magnetic interactions, from extended Hückel calculations,[13] at a maximum of only $J/k_B = -6.98$ K along the direction of the strongest anion···cation interaction, as mediated by S···S contacts. The interaction in **1** should be much weaker.

For **1** the imaginary component of the ac magnetization, with a drive field of 1 Oe and within the 1−20 kHz frequency range (see Figure 5), shows a clear peak at 6.6 K which does not change position with frequency. This shows that the magnetic order below $T_c = 6.6$ K is not due to a glassy or superparamagnetic state but is in fact due to bulk spontaneous magnetization. Furthermore, at 2 K there is magnetic hysteresis (Figure 6 inset) with a rather small coercive field of 66 G and a remnant magnetization of 0.03 $N\beta$.

In the magnetization versus field measurement below T_c, saturation is not reached at 7 T (Figure 6) but reaches a maximum of 3.3 $N\beta$; the value should be 2.0 $N\beta$ if all the $S_{Cr} = 3/2$ spins were oppositely aligned to the $S_{TTF} = 1/2$ spins and 4.0 $N\beta$ if the spins were all aligned in parallel. At 7 T the magnetization is still increasing and looks like it will be asymptotic to 4.0 $N\beta$, which is what is expected if the decoupling occurs. This is self-consistent with the χ_m versus T curves at two different fields. Another explanation of the data would be a spin flop at some low field as in (BDH-TTP)[Cr(NCS)$_4$(isoquinoline)],[9] but there is no change in the gradient of M versus H which can be assigned to this.

(13) Mori, T.; Katshuhara, *J. Phys. Soc. Jpn*. **2003**, *72*, 149.

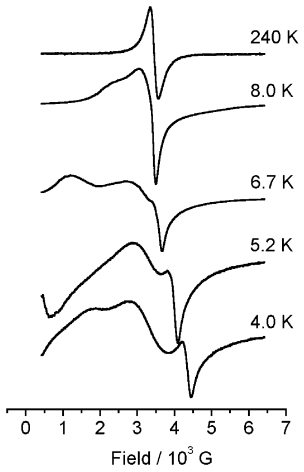

Figure 7. X-band EPR spectra of salt **1** at different temperatures from 240 to 4.0 K.

Compound **1** is the first TTF-based radical cation salt to have this kind of induced paramagnetic behavior, since all other $\pi-$d magnets have either a simple ferrimagnetism or a weak ferromagnetism. However, more detailed magnetic measurements need to be done to confirm this assignment. In particular single-crystal measurements would be very informative by comparing the magnetization along the easy axis with that perpendicular to it, where a spin flop would be more easily seen. At the moment no suitable crystals have been made, but work will continue in this area. Nevertheless, the structural differences in comparison with [BEDT-TTF]-[Cr(NCS)$_4$(isoquinoline)$_2$][7] are consistent with a weaker interaction between anion and cations that allows the decoupling of the spins when a moderate external field is applied.

An EPR study was carried out on a microcrystalline sample from room temperature to 4.2 K. At room temperature a single broad signal was observed with a g-value of 1.990 and a line width of 246 G. This indicates that there is exchange interaction between the spins of both Cr and TM-TTF spin carrying units since the individual contributions from the cation and anion are not seen separately, as in most other radical cation salts of TTF derivatives with magnetic anions. The g-value is close to that found for the Cr^{3+} ion (1.999) in $K_3[Cr(CN)_6]$.[14] On a decrease of the temperature, new very broad and complex EPR signals appear below 8 K, probably due to an increase in the interactions between the anion and cation spins (Figure 7). The new signals are first observed when the temperature is close to T_c, as measured by ac magnetization. Moreover, it can be noted that upon cooling there is a strong dependence of the g-factor for the major signal on the temperature (Figure 8). Although the g-factor remains practically constant over a wide range of temperatures, at around 12 K it begins to fluctuate and at 6.7 K, very close to T_c, it decreases abruptly to 1.582 at 4 K. This shift in the g-factor is due to the internal magnetic field induced below T_c by the spontaneous magnetization of salt **1**, which can be estimated to be around 890 G.

(14) Baker, J. M.; Bleaney, B.; Bowers, K. D. *Proc. Phys. Soc*. **1956**, *B69*, 1205.

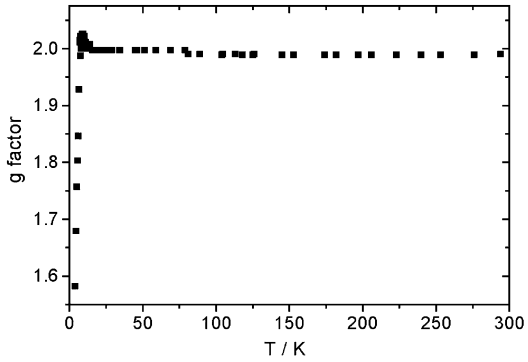

Figure 8. Temperature dependence of the EPR *g*-value of salt **1**.

Conclusions

A new organic−inorganic hybrid salt [TM-TTF][Cr(NCS)$_4$(isoquinoline)$_2$] has been prepared and studied both from a structural and magnetic point of view. The resolution of its crystal structure at five different temperatures from 213 to 123 K shows that there is a phase transition in the crystal structure between 130 and 123 K resulting in stronger interactions between anions and cations. The crystal modification that we suppose occurs at lower temperature does seem to have an effect albeit a small one on the magnetic properties of the title compound. While at room temperature the anions are weakly spin paired, at low temperature ferrimagnetic interaction becomes dominant and gives rise to a bulk spontaneous magnetization in a weak external field. The EPR measurements also demonstrate the interaction between the d and π electrons and the presence of an internal magnetic field brought about by the magnetic ordering at low temperature. However, in a moderate field of 1 T the magnetic data are consistent with decoupling of the spins. Further work will concentrate on preparing new salts of this family, since it has been shown that these anions can promote $\pi-\pi$ interactions between the anion and cation counterpart of their salts, yielding new compounds with unusual magnetic properties, opening new horizons in this field. Furthermore, we are beginning to use different techniques to further understand the magnetic properties of this unusual series, in particular muon spin relaxation and neutron diffraction.

Acknowledgment. This work was supported by the grants from the EC (TMR, ERBFMRX-CT980181) COST action D14/0003/99, DGI-Spain (BQU2000-1157), and DURSI-Catalunya (2001SGR-00362). The work at the Royal Institution is supported by the U.K. Engineering and Physical Sciences Research Council. We thank V. Laukhin for the conductivity measurements and D. Ruiz and S. Carling for useful discussion about magnetism.

Supporting Information Available: X-ray crystallographic files in CIF and pdf formats. This material is available free of charge via the Internet at http://pubs.acs.org.

IC034379C